

LOW-TEMPERATURE SINTERING OF HIGH VOLTAGE GRADIENT ZnO-BASED THICK FILM VARISTORS

LEI KE, DONGMEI JIANG, XUEMING MA

State Key Laboratory of Precision Spectroscopy (East China Normal University),
Department of Physics, East China Normal University, Shanghai 200062, P. R. China

E-mail: kelei@ecnu.cn

Submitted September 23, 2008; accepted January 12, 2009

Keywords: ZnO; thick film varistors; low-temperature sintering; voltage gradient

High voltage gradient ZnO-based thick film varistors were fabricated by low-temperature sintering. The effect of sintering temperature on electrical properties of thick film varistors was investigated. The voltage gradient of thick film varistors increased significantly to 3159.4 V/mm after sintering at 725°C for 30 min. The small average grain size with good grain boundaries was the origin for the increase in voltage gradient. Sample sintered at 725°C exhibited excellent electrical properties, with a leakage current of 36.4 μ A, a nonlinear exponent of 13.1 and the maximum resistivity difference between ZnO grain and grain boundary. Moreover, it possessed high permittivity and low dissipation factor in the low frequency range for the sample sintered at 725°C. Therefore, ZnO-based thick film varistors with high voltage gradient and good nonlinear properties could be obtained under the given experimental conditions and qualified as excellent candidates for high voltage varistor application.

INTRODUCTION

ZnO-based varistors are ceramic semiconductor devices, which have been widely used in voltage stabilization, transient surge protection in electronic circuits and electrical power systems [1]. They exhibit excellent nonlinear current-voltage (I-V) characteristics expressed by $I = KV^\alpha$, where K is a constant that depends on the microstructure and α is the nonlinear exponent. Recently, there has been considerable demand recently for varistors being miniaturization and integration with high voltage gradient [2]. Conventional ZnO-based varistors are ceramic blocks and cannot meet the need of some specific application such as surface mount devices, varistors array, etc. Because of mass production at low cost and versatility in the design, ZnO-based thick film varistors (TFVs) appear to become suitable substitutes and attract more and more public attention [3-5].

Until now, various techniques [4-8] have been employed to prepare ZnO-based TFVs, mainly including sol-gel method, tape casting, direct-write technique, screen-printing and so on. Barrow et al. [6] prepared TFVs by sol-gel method with the film thickness of 200 μ m under the sintering temperature of 1000°C. Rubia et al. [7] obtained the ZnO-based TFVs with a high voltage gradient value above 2000 V/mm by tape casting for a sintering temperature of 950°C. Tovher et al. [5] reported that ZnO-based TFVs could be sintered at low temperature of 900°C. They fabricated ZnO-based TFVs by direct-write technique with Na and Al dopants and the value of voltage gradient reached 1200 V/mm.

However, due to their complex experiment processes and high costs, it is difficult for these techniques to realize the final aim of industrialization. Menil et al. [4] prepared ZnO-based TFVs by screen-printing with the sintering temperature of 1150°C and the voltage gradient value was 900 V/mm. Rubia et al. [8] proposed a method to improve the voltage gradient by replacing Sb_2O_3 and Bi_2O_3 with the equivalent amount of a $Zn_7Sb_2O_{12}$ orthorhombic spinel phase and a $Bi_{38}ZnO_{58}$ sillenite phase previously synthesized, respectively. The screen-printed samples were sintered at 900°C and the voltage gradient value was beyond 1000 V/mm. Although both two methods have obvious advantages in low costs and simple techniques by screen-printing, it is difficult to apply the products to high voltage field because of their low voltage gradient resulted from the high sintering temperature.

In most of previous reports [2-4, 7, 9] on screen-printed ZnO-based TFVs, sintering temperatures were higher than 850°C which made the grain size become larger after annealing process. The decrease of grain boundary amount and large volatilization of Bi_2O_3 reduced the voltage gradient of TFVs and resulted in the deterioration failure of grain boundaries, leading the nonlinear properties to be disappeared. However, high activity of fine particles with a nearly equiaxed grain morphology, which had been reduced by high-energy ball milling in the initial period of experiment, was reported to reduce sintering temperature [10-11]. In this study, high voltage gradient ZnO-based TFVs were fabricated with smooth surfaces and good adhesion by screen-printing.

ting with low sintering temperatures between 650 and 850°C. The potential of the fabrication technology as viable and cost effective manufacturing route was demonstrated. More importantly, the effects of sintering temperature on microstructure, current-voltage characteristics and dielectric characteristics of TFVs were presented and discussed.

EXPERIMENTAL

Reagent-grade raw materials were used in proportions of 96.42 mol.% ZnO + 0.7 mol.% Bi₂O₃ + 1.0 mol.% Sb₂O₃ + 0.5 mol.% Cr₂O₃ + 0.8 mol.% Co₂O₃ + 0.5 mol.% MnO₂ + 0.08 mol.% Y₂O₃. The materials were mixed in a planetary ball mill for 5 h with a stainless steel grinding media and ethanol as a mixing vehicle. The mixture was dried at 120°C for 2 h and pulverized using an agate mortar/pestle. The thick film pastes were prepared by adding 80 wt.% of powders to an organic vehicle and mixing them for 30 min. The organic vehicle, based on terpineol as the solvent, ethyl cellulose as the binder and rheological modifier, and acetylacetone as the dispersant were selected for the paste preparation. Then TFVs were obtained by sequentially screen-printing the bottom electrode, the thick film layers and the top electrode on a 99.6 % alumina substrate. Commercial silver paste (Baoyin, BY-6070) was used for the electrodes and the final thickness of TFVs was controlled by the screen-printing times. The samples were dried at 120°C to initially eliminate the organic solvents and then sintered at nine different temperatures from 650 to 850°C for 30 min with a heating rate of 5°C/min after soaking at 500°C for 30 min to remove the remaining organics.

The crystalline phases of ZnO-based TFVs were studied using X-ray diffractometry (XRD, D/max 2550V). The microstructure of TFVs was examined with scanning electron microscopy (SEM, JSM-5610LV). The average grain size (D) was determined by the measurement on the micrographs with the linear intercept method [12-14] using the expression $D = 1.56 L/MN$, where L is the randomline length on the micrograph, M is the magnification of the micrograph, and N is the number of the grain boundaries intercepted by lines. The density of the sintered TFVs was estimated [15] from the micrographs by calculating the ratio of the grains and void areas and then transforming the area ratio (R_{area}) to the corresponding volumetric ratio ($R_{\text{volume}} = R_{\text{area}}^{3/2}$). The area of voids was differentiated from the area of grains in the micrographs by their difference in tonal values. The electrical properties of TFVs were measured from a CJ1001 varistor DC parameter testing instrument. The breakdown voltage ($U_{1\text{mA}}$) was measured at the current density of 1.0 mA/cm² and the voltage gradient ($E_{1\text{mA}}$) was obtained by $E_{1\text{mA}} = U_{1\text{mA}}/d$, where d is the thickness of sample. The leakage current (I_L) was measured at the electrical field of 0.75 $U_{1\text{mA}}$ and the nonlinear coef-

ficient (α) was determined in the range of 1.0 mA/cm² to 10 mA/cm² in current density, according to the expression of $\alpha = 1/(\log E_{10\text{mA}} - \log E_{1\text{mA}})$. The instrument also contained a DC power supply so as to describe the I-V characteristics. The dielectric parameters of TFVs, including the permittivity (ϵ_r), the dissipation factor ($\tan \delta$) and the resistivity ($|Z|$), were measured using a precision impedance analyzer (PIA, Agilent 4294A) in the frequency range of 10² ~ 10⁷ Hz.

RESULTS AND DISCUSSION

Figure 1 shows the electrical parameters of ZnO-based TFVs with different sintering temperatures. As can be seen in Figure 1a, the $E_{1\text{mA}}$ value is significantly affected by sintering temperature. With the increase of sintering temperature, $E_{1\text{mA}}$ increases at first and then decreases. The value of $E_{1\text{mA}}$ achieves maximum of 3159.4 V/mm in the sample sintered at 725°C. Increasing sintering temperature further causes the $E_{1\text{mA}}$ value to decrease, whereas all samples exhibit a high voltage gradient, which is beyond 2600 V/mm. Figure 1b and c show the variation of I_L and α with different sintering temperatures. On the whole, the variation of I_L is opposite to that of α . The measured extrema of I_L and α are 36.4 μA and 13.1 for the sample sintered at 725°C. The effects on I_L and α with different sintering temperatures are similar to that on $E_{1\text{mA}}$. Samples with better $E_{1\text{mA}}$, I_L and α are obtained in the optimum sintering temperature region, almost between 725-800°C. Once beyond this range, $E_{1\text{mA}}$ and α decrease abruptly with I_L increasing acutely. Therefore, the electrical properties of ZnO-based TFVs were greatly affected with the increase of sintering temperature. It accelerates the deterioration in $E_{1\text{mA}}$, as well as I_L and α , when the samples are sintered beyond the certain temperature range of 725-800°C.

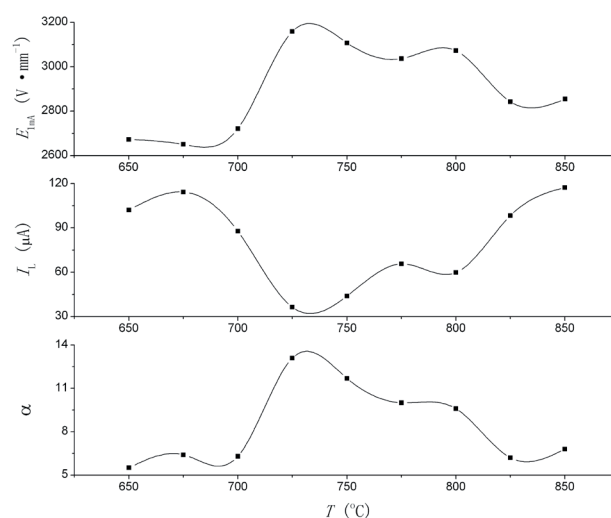


Figure 1. Evolution of electrical parameters as functions of sintering temperature.

For further analyses about the structural and electrical properties of ZnO-based TFVs, four samples sintered at 675, 725, 775 and 825°C are selected. Figure 2 shows the SEM micrographs of four samples sintered at different temperatures. It can be intuitively seen that the grain size increases and the pore size decreases with increasing sintering temperature. As the sintering temperature is raised from 675 to 825°C, the average grain size has an increase from 1.032 to 1.414 μm . All the sintered samples show a somewhat porous microstructure. The estimated density values are 71, 78, 76 and 78 vol.% for the samples sintered at 675, 725, 775 and 825°C, respectively. Although the densities evaluated from the SEM micrographs cannot be considered as absolute values, they can be used to compare the film densities. A gradual increase in densification is seen with increasing sintering temperature. The microstructures and estimated density values show that, in the preparation conditions we used, higher density samples are obtained with sintering temperatures of 725, 775 and 825°C. Sample sintered at 675°C has a looser structure with big holes, which inevitably affects the electrical properties.

However, more research is needed in order to study the effects of sintering conditions on the density of ZnO-based TFVs.

The phase composition of ZnO-based TFVs is shown in Figure 3. The XRD patterns clearly indicate that all the prepared samples except for the sample sintered at 675°C are composed of ZnO phase, $\text{Zn}_7\text{Sb}_2\text{O}_{12}$ phase and Bi_2O_3 phase. No $\text{Zn}_7\text{Sb}_2\text{O}_{12}$ phase is observed in the sample sintered at 675°C. An early sintering study [16] indicates that the formation temperature of $\text{Zn}_7\text{Sb}_2\text{O}_{12}$ phase in ZnO-based systems is above 700°C and the deliquescent $\text{Zn}_7\text{Sb}_2\text{O}_{12}$ particles between ZnO grains can restrain the grain growth. The sintering temperature of 675°C is so low that it is difficult to form $\text{Zn}_7\text{Sb}_2\text{O}_{12}$ phase under this condition. The appearance of $\text{Zn}_7\text{Sb}_2\text{O}_{12}$ phase above 700°C coexists with Bi_2O_3 phase and plays a distribution role in phase composition. Therefore, the grain boundaries for the sample sintered at 675°C are not formed well. However, increasing sintering temperature weakens the diffraction peak intensity of Bi_2O_3 phase. The peak intensity of Bi_2O_3 phase for the sample sintered at 825°C is obviously less

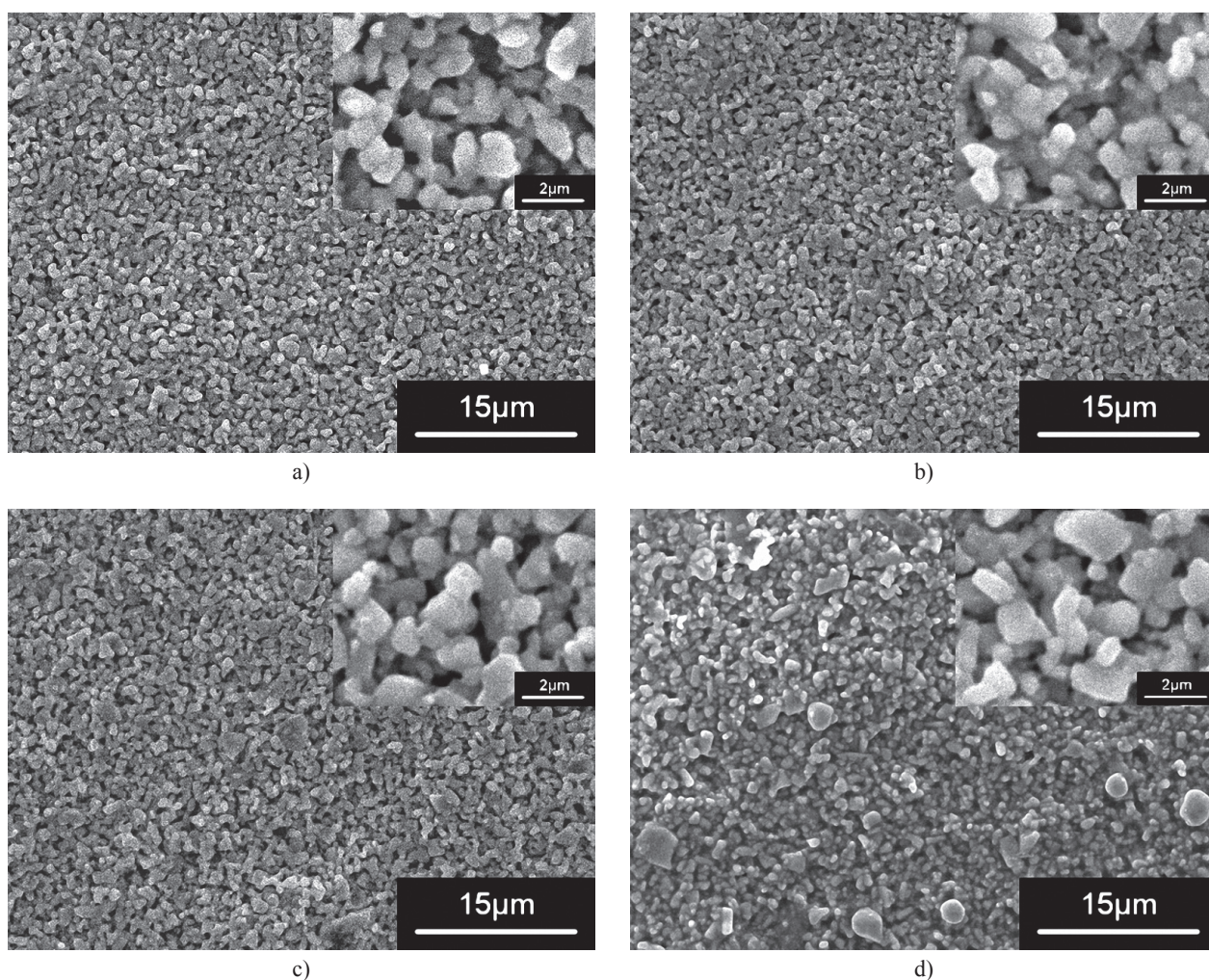


Figure 2. SEM micrographs of four samples with different sintering temperatures; a) 675°C, b) 725°C, c) 775°C and d) 825°C.

than that sintered at 675, 725 and 775°C, which is due to the partial volatilization of Bi₂O₃. The loss of Bi₂O₃ phase for the sample sintered 825°C inevitably results in the decrease of nonlinearity. Because of the detection limit of XRD equipment, small amounts of other additives, such as Cr₂O₃, Co₂O₃, MnO₂, Y₂O₃, are not detected.

The I-V characterization of these samples normalized in electrical potential gradient (E) as a function of current density (J) is shown in Figure 4. It shows that the conduction characteristics are divided into two regions: prebreakdown region at low electric field and break-down region at high electric field. The knee of curves between the two regions plays an important role in electrical behaviors of ZnO-based TFVs. In other words, the better nonlinearity can be obtained with the sharper knee. Samples sintered at 725 and 775°C exhibit nearly similar shape of characteristic curves and show higher nonlinearity. However, it can be forecasted that samples sintered at 675 and 825°C exhibit the worse nonlinear properties by showing nearly round-like knee. The detailed I-V characteristics parameters, including the barrier height (Φ_B), depletion layer width (t), donor density (N_D) and density of interface states (N_S) are summarized in Table 1. Φ_B and t are determined by the thermionic emission theory [17] described as $\ln J = \beta^{1/2}/kT + \ln A^* T^2 - \Phi_B/kT$, where $\beta \propto 1/t$ is a constant governed

by depletion layer width, k is Boltzmann's constant, T is absolute temperature and A^* is Richardson's constant. N_D and N_S are determined by the equations $N_D = 2\varepsilon\Phi_B/e^2t^2$ and $N_S = N_D/t$, where ε is the permittivity of ZnO ($\varepsilon = 8.5 \varepsilon_0$) and e is the charge of a single electron. Calculated from the J-E curves in Figure 4, Φ_B , N_D and N_S coincide with the variation of E_{1mA} values in I-V characteristics, while t shows opposite relation to E_{1mA} . The Φ_B value increases from 0.70 to 0.81 eV between 675 and 725°C, whereas it decreases to 0.71 eV with further increasing sintering temperature to 825°C. As the sintering temperature increases, the t value decreases to a minimum value of 10.2 nm in the sample sintered at 725°C. Increasing sintering temperature further causes the t value to increase. The variations of Φ_B and t result from the Schottky barrier at grain boundary. High and narrow barrier formed at the sintering temperatures of 725°C is helpful to improve the electrical properties of ZnO-based TFVs, especially in E_{1mA} and α . At the sintering temperature of 675°C, the average value of voltage across single grain/grain boundary (U_g) is 2.74 V, which can be estimated by the equation $U_g = E_{1mA} D$. Lower U_g value also shows that the grain boundary formed at this temperature is not good and results in the poor nonlinear properties. At higher sintering temperatures of 825°C, although the average value of U_g achieves a high level of ~ 4 V, the loss of Bi₂O₃ combined with low and wide barrier causes the electronic inactivity of grain boundaries and deteriorates the nonlinear properties.

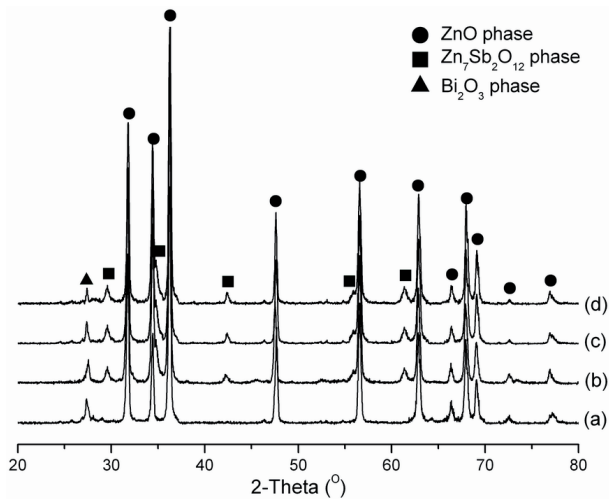


Figure 3. XRD data of four samples with different sintering temperatures; a) 675°C, b) 725°C, c) 775°C and d) 825°C.

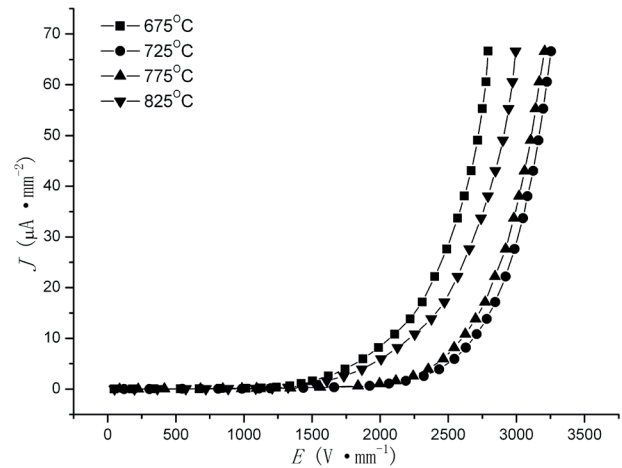


Figure 4. Partial J-E curves for the four samples.

Table 1. Experiment parameters of ZnO-based TFV for different sintering temperatures^a.

T (°C)	(E_{1mA}) (V/mm)	I_L (μA)	α	D (μm)	U_g (V)	Φ_B (eV)	t (nm)	N_D ($\times 10^{18}/cm^3$)	N_S ($\times 10^{12}/cm^2$)
675	2650.8	114.3	6.4	1.032	2.74	0.70	32.9	0.61	2.00
725	3159.4	36.4	13.1	1.290	4.08	0.81	10.2	7.34	7.49
775	3036.2	65.7	10.0	1.353	4.11	0.75	21.5	1.53	3.28
825	2842.3	98.4	6.2	1.414	4.02	0.71	31.4	0.68	2.14

^a T: sintering temperature

Figure 5 shows the frequency variation of dielectric parameters of ZnO-based TFVs sintered at various temperatures. It is apparent in Figure 5 a that sample sintered at 725°C possesses the highest permittivity (ϵ_r) in the measuring frequency range. The ϵ_r value has

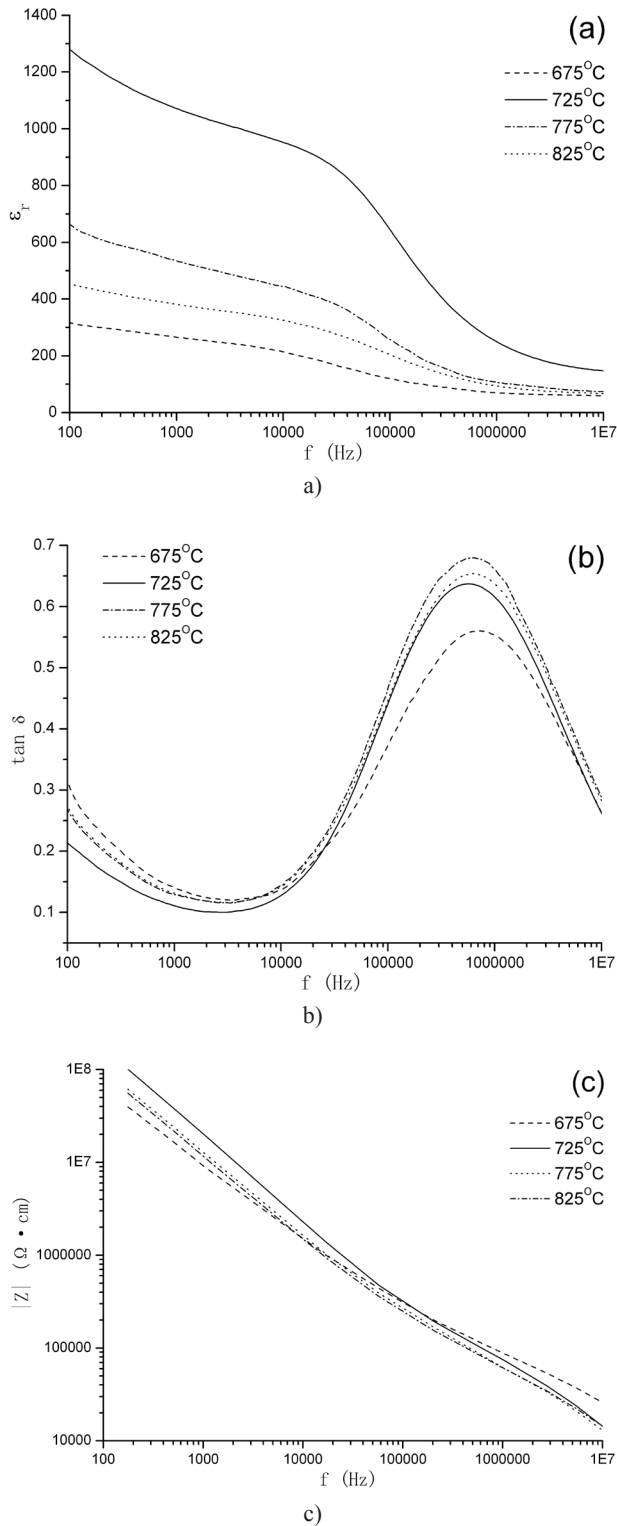


Figure 5. Dielectric properties for the four samples; a) $\epsilon_r - f$, b) $\tan \delta - f$ and c) $|Z| - f$.

little variation as the frequency increases in the range of 10² ~ 10⁴ Hz, while it decreases with a sharper dispersive drop being evident at 10⁵ Hz. In the low frequency range, the effective capacitance is originated from grain boundaries. High ϵ_r with little variation in the low frequency range indicates that the grain boundary formed at 725°C is good. At the high frequency of 10⁵ Hz, the ϵ_r value decreases sharply, which is attributed to the polarization generated in the narrow grain boundaries. With the further increasing of frequency, the ZnO grain capacitance gradually plays a dominant role in ϵ_r . With the increase of sintering temperature, ϵ_r increases at first and then decreases, which is due to the grain boundary layer capacitance (GBLC) effect [18-19]. According to the simple series model for the GBLC effect, ϵ_r of ZnO-based TFVs can be simply expressed as $\epsilon_r = \epsilon(D/t)$, where ϵ is the permittivity of ZnO, D is average grain size and t is depletion layer width. In these samples, D increases gradually and t exhibits a minimum value as the sintering temperature increases, as shown in Table 1. The equation $\epsilon_r = \epsilon(D/t)$ indicates that ϵ_r can be controlled by the thin insulative depletion layer and the average grain size, which is opposite to the thickness of depletion layer and proportional to the average grain size. Compared with the slow growth in grain size, the influence of the thickness of depletion layer on ϵ_r is more remarkable. Therefore, although the average grain size of ZnO-based TFVs increases with increasing sintering temperature beyond 725°C, the thickness of depletion layer also increases, which leads to a decrease of ϵ_r . It is found in Figure 5b that the values of dissipation factor ($\tan \delta$) are also greatly affected by sintering temperature. All the TFVs exhibit an obviously dispersion with the increasing frequency from 10² to 10⁴ Hz and the sample sintered at 725°C has the lowest $\tan \delta$. In the low frequency range, the dielectric loss mainly depends on electric conductance and is determined by the grain boundary resistance. Lower $\tan \delta$ value indicates that the grain boundaries formed at 725°C are better than that formed at others sintering temperatures, which has also been proved by the lower I_L for the sample sintered at 725°C. In addition, the dielectric loss peak of all the TFVs can be seen clearly through $\tan \delta - f$ curve at ~10⁶ Hz. This is strongly affected by polarization loss in the high frequency range. Levinson et al. [20] considered the dielectric loss peak is originated from the polarization of thermion. The material components and process conditions also have important effects on the dielectric loss peak. Figure 5c shows the variation in resistivity ($|Z|$) of ZnO-based TFVs with different sintering temperatures. The results reveal that as the measuring frequency increases, $|Z|$ of all the samples decreases significantly with a nearly logarithm linear relation on f . The $|Z|$ values of ZnO-based TFVs achieve ~10⁷ Ωcm at 10³ Hz and decrease in several orders of magnitude as the frequency increases in the range of 10²~10⁷ Hz. The resistivity of grain boundary plays the

leading role in the low frequency range, while the grain resistivity takes a leading position in the high frequency range. The difference of $|Z|$ between low frequency range and high frequency range actually represents the resistivity difference of grain boundary and ZnO grain. Although the $|Z|$ - f curves overlap or closely approach, it can be seen in the Figure 6 that sample sintered at 725°C has the maximum resistivity difference and sample sintered at 675°C has the minimum resistivity difference. Therefore, due to the higher resistivity difference, sample sintered at 725°C possesses the good grain boundary characteristics with lower I_L and higher α , as shown in Table 1.

CONCLUSIONS

High voltage gradient ZnO-based TFVs are fabricated by sintering at a low temperature region from 650 to 850°C. The electrical properties of TFVs are investigated with various sintering temperatures. Sample with excellent electrical properties is obtained at the sintering temperature of 725°C, which exhibits a E_{1mA} value of 3159.4 V/mm, a I_L value of 36.4 μ A and a α value of 13.1.

Under the given experimental conditions, small average grain size is the origin for the increase in voltage gradient. As the sintering temperature is raised from 675 to 825°C, the average grain size has a little increase from 1.032 to 1.414 μ m. High and narrow grain boundary barrier formed at the sintering temperatures of 725°C improves the grain boundary properties. In addition, high ϵ_r with little variation and low $\tan\delta$ in the low frequency range indicate that the grain boundaries formed at 725°C are better. The maximum resistivity difference between ZnO grain and grain boundary in the measuring frequency range is also obtained at the sintering temperature of 725°C, which directly results in the good nonlinearity.

Acknowledgement

The authors would like to acknowledge the financial support of the Nano Special Plan from Shanghai Municipal Science and Technology Plan of Commission

(Grant No. 0852nm06000) and Shanghai Municipal Natural Science Foundation (Grant No. 08ZR1406700).

References

1. Clarke D. R.: J. Am. Ceram. Soc. 82, 485 (1999).
2. Lucat C., Martin M. P., Debéda H., Largeteau A., Ménéil F.: J. Eur. Ceram. Soc. 27, 3883 (2007).
3. Debéda H., Lucat C., Ménéil F.: J. Eur. Ceram. Soc. 25, 2115 (2005).
4. Ménéil F., Debéda H., Lucat C.: J. Eur. Ceram. Soc. 25, 2105 (2005).
5. Tohver V., Morissette S. L., Lewis J. A.: J. Am. Ceram. Soc. 85, 123 (2002).
6. Barrow D. A., Petroff T. E., Sayer M.: Surf. Coat. Tech. 76-77, 113 (1995).
7. De la Rubia M. A., Peiteado M., De Frutos J., Rubio F., Fernández J. F., Caballero A. C.: J. Eur. Ceram. Soc. 27, 3887 (2007).
8. De la Rubia M. A., Peiteado M., Fernández J. F., Caballero A. C., Holc J., Drnovsek S., Kuscer D., Macek S., Kosec M.: J. Eur. Ceram. Soc. 26, 2985 (2006).
9. Stolz S., Bauer W., Ritzhaupt H. J., Haufelt J.: J. Eur. Ceram. Soc. 24, 1087 (2004).
10. Fah C. P., Wang J.: Solid State Ionics 132, 107 (2000).
11. Alamdari H. D., Boily S., Blouin M.: Mater. Sci. Forum 343-346, 909 (2000).
12. Güntürkün K., Toplan H. Ö.: Ceramics-Silikáty 50, 225 (2006).
13. Toplan H. Ö., Erkalpa H., Özkan O. T.: Ceramics-Silikáty 47, 116 (2003).
14. Wurst J. C., Nelson J. A.: J. Am. Ceram. Soc. 55, 109 (1972).
15. Tick T., Peräntie J., Jantunen H., Uusimäki A.: J. Eur. Ceram. Soc. 28, 837 (2008).
16. Inada M.: Jpn. J. Appl. Phys. 19, 409 (1980).
17. Eda K.: J. Appl. Phys. 49, 2946 (1978).
18. Cai J. N., Lin Y. H., Li M., Nan C. W., He J. L., Yuan F. L.: J. Am. Ceram. Soc. 90, 291 (2007).
19. Wu J., Nan C. W., Lin Y. H., Deng Y.: Phys. Rev. Lett. 89, 217601 (2002).
20. Levinson L. M., Philipp H. R.: J. Appl. Phys. 47, 1117 (1976).